

Transmittance and optical constants of Sr films in the 6-1,220 eV spectral range

Luis Rodríguez-de Marcos, Juan I. Larruquert^a, José A. Aznárez, Manuela Vidal-Dasilva, Sergio García-Cortés, José A. Méndez

GOLD-Instituto de Óptica-Consejo Superior de Investigaciones Científicas

Serrano 144, 28006 Madrid, Spain

Luca Poletto, Fabio Frassetto

Institute of Photonics and Nanotechnologies-National Council for Research,

via Trasea 7, 35131 Padova, Italy

A. Marco Malvezzi, Daniele Bajoni

Dipartimento di Elettronica, Università di Pavia and Consorzio Nazionale Interuniversitario per le

Scienze Fisiche della Materia, Via Ferrata, 1, I27100 Pavia, Italy

Angelo Giglia, Nicola Mahne

Istituto Officina dei Materiali Istituto Officina dei Materiali-Consiglio Nazionale delle Ricerche

Laboratorio Tecnologie Avanzate e NanoSCienza, Area Science Park Basovizza, S.S. 14 Km 163.5,

34149 Trieste, Italy

Stefano Nannarone

Dipartimento di Ingegneria dei Materiali e dell Ambiente, Università di Modena e Reggio Emilia,

Via Vignolese 905, I-41100 Modena, Italy

ABSTRACT

Strontium (Sr) is a material with low-absorption bands in the extreme ultraviolet (EUV), which makes it a potential candidate for band pass filters and multilayer coatings. Yet, a better knowledge

^a Author to whom correspondence should be addressed. Electronic mail: larruquert@ifa.cetef.csic.es; fax number: 34 914117651

of the optical properties of Sr is required for these developments. The optical constants n and k of Sr thin films have been obtained in the 6-1220 eV range from transmittance measurements performed at room temperature. These are the first experimental optical constant data of Sr in most of the range. Thin films of Sr with various thicknesses were deposited by evaporation in ultrahigh vacuum conditions and their transmittance was measured *in situ*. Sr films were deposited onto grids coated with a thin C support film. Transmittance measurements were used to directly obtain the extinction coefficient k of Sr films. The refractive index n of Sr was calculated with Kramers-Kronig analysis. For this, k data were extrapolated both on the high- and on the low-energy sides by using experimental and calculated k data available in the literature. It was found that, similar to other alkaline-earth metals, Sr has a low absorption band in the EUV below its N_{2,3} edge, with a minimum at ~18.5 eV, a range where most materials in nature have a large absorption. A second spectral range of interest for the low absorption of Sr is below its M_{4,5} edge at 132 eV. In spite of these remarkable properties, Sr is a very reactive material and the stability of coatings encompassing Sr may be an issue. Good consistency of the data resulted from the application of f and inertial sum rules.

Keywords: Extreme Ultraviolet; Far Ultraviolet; Optical constants; Absorption filters; Multilayers; Optical properties of thin films

1. INTRODUCTION

The development of efficient coatings for the extreme ultraviolet (EUV) requires the availability of materials with low absorption. The EUV data available suggest that alkaline-earth metals^{1, 2, 3, 4} have low-absorption bands in parts of the EUV, which makes alkaline-earths promising materials for multilayer coatings or absorption filters. Their low-absorption in the long wavelengths of the EUV, particularly of Sr and Ba¹, is shared also by lanthanides, which have been recently characterized in a broad range including the EUV: La^{5, 6}, Ce⁷, Pr⁸, Nd⁶, Sm⁹, Eu¹⁰, Gd⁶, Tb^{5, 6}, Dy⁶, Ho^{9, 11}, Er^{9, 12}, Tm¹³, Yb^{14, 15}, and Lu¹⁶, along with materials with close properties such as Sc^{17, 18, 19, 20}, and Y²¹.

Few data on the optical constants of Sr were found in the literature. From these data it is remarkable the research of Endriz and Spicer¹, who measured the reflectance of thin films deposited by evaporation in the 0.3-11.6 eV range and calculated the optical constants of Sr with Kramers-Krönig (KK) analysis. Other than this, various authors reported absorption spectra of Sr vapour: Mansfield *et al.*²² in 130-310 eV, Brown *et al.*²³ in 6.54-8.87 eV, Garton *et al.*²⁴ in 5.1-7.5 eV, and Hudson *et al.*²⁵ in 6.12-7.54 eV. Aymar *et al.*²⁶ reported the absolute photoabsorption cross section of Sr vapour in the 8.69-11.92 eV range.

Other than optical measurements, Langkowski²⁷ measured electron energy-loss spectra of Sr thin films in the 2-50 eV range and calculated the complex dielectric function in the same range. Ley *et al.*²⁸ reported the x-ray core spectra of Sr films measured by x-ray photoemission spectroscopy. Kanski *et al.*²⁹ performed appearance potential spectra for alkaline-earth metals Ca, Sr and Ba; they reported data of Sr in the M_{4,5} edge. Mende *et al.*³⁰ reported oscillator strengths of transitions into high-lying Rydberg states (5.66-5.69 eV) of the Sr I principal series. Henke *et al.*³¹ obtained a semiempirical set of data in the 30-10000 eV range (later extended to 30000 eV)³². In their calculation, they used Mansfield data²².

In view of the incomplete data in the literature, this paper is aimed at providing accurate optical data on pure Sr films in a broad spectral range. This paper addresses the optical properties of Sr films in the 6-1220 eV range. The optical properties in this energy range are characterized by the presence of three intense absorption bands $M_{2,3}$, $M_{4,5}$ and $N_{2,3}$, in order of decreasing energy and by the presence of a weak M_1 band, due to the excitation of 3p, 3d, 4p, 3s electron, respectively. It is organized as follows. A brief description of the experimental techniques used in this research is given in Sec. II. Section III presents transmittance data of Sr films, the extinction coefficient calculated from transmittance, and the dispersion obtained using KK analysis; the consistency of the data gathered in this research is also evaluated.

2. Experimental techniques

2.1 SAMPLE PREPARATION

Both Sr film deposition and characterization were performed under ultrahigh vacuum (UHV) at Bending Magnet for Emission Absorption and Reflectivity (BEAR) beamline of ELETTRA synchrotron (Trieste, Italy). Sr films were deposited onto 5-nm thick C films supported on 117-mesh Ni grids with 88.6% nominal open area (pitch of 216 μm). The procedure for C film preparation was reported elsewhere³³. Sr films were deposited with a TriCon evaporation source³⁴, in which a small Ta crucible filled with Sr is bombarded by electrons that impinge on the crucible wall. Sr granules of 99.9% purity, which were provided sealed in cans under argon by ESPI Metals, were used. The crucible-sample distance was 200 mm. Deposition rate was ~ 4 and ~ 9 nm/min for the thinner and the thicker samples, respectively. Film thickness was monitored with a quartz crystal microbalance during deposition. Sr films were deposited onto room-temperature substrates. A witness glass substrate was placed close to the grid-supported C film to get coated simultaneously with a similar Sr film thickness. Reflectance versus the incidence angle was measured on the witness samples at the energy of 115 eV and the angular positions of the minima and maxima were used to calculate the Sr

film thickness; the distance between the areas of transmittance and reflectance measurements was less than 10 mm. Since reflectance measurements were performed far from absorption edges, Henke optical constants^{31,32} could be used in this calculation. Henke data were downloaded from the website of the Center of X-Ray Optics (CXRO) at Lawrence Berkeley National Laboratory³⁵.

2.2 EXPERIMENTAL SETUP FOR TRANSMITTANCE MEASUREMENTS

Transmittance measurements were performed at BEAR beamline with vertical slits of 100 μm above 24 eV and 450 μm below 24 eV; the monochromator spectral resolution $E/\Delta E$ varied between 500 and 2000, depending on slit widths. The suppression of higher orders was achieved using quartz, LiF, In, Sn, Al, and Si filters at specific ranges below 100 eV, and choosing a plane mirror-to-grating deviation angle in the monochromator setup that minimized the higher order contribution at energies above 100 eV. The detector was a silicon diode model SXUV-100 from IRD. The beam cross section at the sample was about $0.7 \times 1.5 \text{ mm}^2$.

Measurements were performed in BEAR spectroscopy chamber^{36,37,38}, which operates at a base pressure in the 1×10^{-8} Pa range. Samples were deposited at a pressure of $\sim 2 \times 10^{-6}$ Pa in the preparation chamber, which had a base pressure of $\sim 5 \times 10^{-7}$ Pa. The two chambers are connected in vacuum, which allows sample transfer between the chambers in UHV conditions.

Three C substrates were used and their transmittance was measured previously to Sr deposition. Two, one, and two successive Sr coatings of various thicknesses were accumulated upon the first, the second and the third substrates, respectively, without breaking vacuum. The first and third substrates were transferred back and forth between the deposition chamber and the measurement chamber for the deposition of the second Sr film and their characterization. Transmittance measurements were performed onto samples at room temperature. For each film, uniformity evaluations were performed. At energies above 18 eV, fluctuations of the photon beam during transmittance measurements were

recorded with a 100-V biased Au mesh and with the storage ring current; below 18 eV, only the ring current was available. Beam fluctuations were cancelled by normalizing the recorded beam intensity to the mesh current, or, when the latter was noisy, to the ring current.

3. Results and discussion

3.1 TRANSMITTANCE AND EXTINCTION COEFFICIENT OF Sr

We measured the transmittance of Sr films with the following thicknesses: 21.5 and 31.5 nm on the first substrate, 85.0 nm on the second substrate and finally 39.8 and 64.0 nm on the third substrate. These thicknesses were calculated by fitting reflectance measurements versus angle of incidence to the calculated reflectance using Henke data^{31,32} at the energy of 115 eV. In some cases the fit was somewhat imprecise, so that a second method to determine the film thicknesses was used consisting in the following: the transmittance-versus-energy curve for each film thickness above 60 eV was fitted to the data calculated with Henke's optical constants by varying the film thickness until the best match was obtained; the fitted thickness was taken as the real film thickness. The above thickness data include such a correction.

The transmittance of Sr films normalized to the transmittance of the uncoated substrate is plotted in Fig.1. There are two high transmission bands peaked at ~130 eV and ~18.6 eV, right below Sr M_{4,5} and N_{2,3} edges, respectively. The low-energy band of relative large transmittance extends from approx. 14 to 20 eV. Close transmittance bands have been measured for other alkaline-earth metals and lanthanides; this transmittance band makes Sr a promising material for transmittance filters or multilayer spacers for the EUV in the ~14-20 eV spectral range, where there has been a lack of low-absorbing materials until recently. Slight oscillations were observed that are assigned to the small presence of N (398 eV), Ti (458-464 eV), O (528 eV), and Fe (717 eV); an oscillation at 99.8 eV is explained as an artifact of data normalization due to the abrupt signal decrease at the absorption edge

of the Si filter. At 284-286 eV a larger oscillation was encountered, which is visible in Fig.1, and it is attributed to carbon contamination, either at the optics or on the sample.

If the contribution to transmittance coming from multiple reflections inside the Sr film is negligible, the extinction coefficient k (the imaginary part of the complex refractive index) can be calculated from transmittance with the following equation:

$$\ln\left(\frac{T_{fs}}{T_s}\right) \approx A - \left(\frac{4\pi k}{\lambda}\right) \cdot d \quad (1)$$

where T_s and T_{fs} represent the transmittance of the uncoated substrate and of the substrate coated with a Sr film, respectively; λ is the radiation wavelength in vacuum; d stands for the Sr film thickness. Eq. (1) is a straightforward derivation of the well-known Beer-Lambert law. A is a constant for each energy and encompasses the terms that involve reflectance, in the assumption that multiple reflections are negligible.

The k of Sr films was calculated by fitting the slope of the logarithm of the transmittance versus thickness at each energy using Eq. (1); the data are represented in Fig. 2. The semiempirical data of Henke^{31,32}, also plotted in Fig. 2, were calculated with a density of 2.58 g/cm³. The aforementioned presence of contaminants is less significant on k than on transmittance because samples of different Sr thicknesses with similar presence of contaminants (either on the sample or on the light path), or with artifacts coming from normalization at transmittance calculation, will tend to cancel out in the calculation of k with the slope method. There is an exception on C: it is significant in both transmittance and k ; this can be due to a larger presence of C contamination, which might be related to the high reactivity of Sr.

When reflectance is not negligible, the application of Eq. (1) to calculate k with the slope method may result in uncertainties. In order to overcome this, we proceeded in an iterative way. The iterative method was applied in the 4-104 eV range, and it involved also data extrapolation at smaller energies. For the first iteration, initial k values were obtained using the slope method (except in the

40-130 eV range, which is discussed below). These values, along with k data in the rest of the spectrum, were used to obtain the refractive index n (the real part of the complex refractive index) with KK analysis (KK analysis is described in subsection III.B). Once a first set of data $\{n(E), k(E)\}$ was available, the transmittance ratio of the C/Sr coated substrate to the C uncoated substrate was calculated with the usual equations based on Fresnel coefficients. This transmittance ratio was compared with the measured data; the difference between measured and calculated transmittance gave us an estimate to modify k . This modified value was a second estimate of k , from which a second estimate of n was obtained with KK analysis. Three such iterations were performed until the difference between the experimental and the calculated transmittance data was negligible. The optical constants of the single C film at this same range had been previously calculated with a similar procedure starting with k obtained from the transmittance of an uncoated C substrate.

k values close to $N_{2,3}$ edge are presented in Fig. 3. The smallest value of k is 0.029, which is obtained at ~ 18.5 eV, is remarkable since there is a need for low-absorption materials in this range for optical coatings. This minimum is slightly smaller than the minimum for Eu at its $O_{2,3}$ edge, with a k of 0.042 at ~ 16.6 eV¹⁰. Hence Sr, along with Mg and Al, are among the materials with smallest k in the 16.5-20 eV energy range. This minimum for Sr is close to the ones obtained for rare earths at the following energies: Ce at ~ 16.1 eV, La at ~ 16.5 eV, Eu at ~ 16.6 eV, Pr at 16.87 eV, Nd at ~ 17 eV, Sm at ~ 18.5 eV, Tb at ~ 19.5 eV, Gd at ~ 19.7 eV, Dy at ~ 20.2 eV, Yb at ~ 21.2 eV, Ho at ~ 22 eV, Er at ~ 22.5 eV, Tm at ~ 23 eV, Lu at ~ 25.1 eV and Sc at ~ 27 eV. As aforementioned, this low-absorption of Sr in this range is promising for its use in transmittance filters or reflective multilayers. However, Sr is a very reactive material, and this may result in the need to develop protective or barrier layers for Sr.

k at $M_{4,5}$ and $M_{2,3}$ edges is presented in Fig. 4, along with the semiempirical data of Henke^{31,32}. The presence of C can be seen through its K edge. The low absorption of Sr below its $M_{4,5}$ edge at 132 eV results in a second spectral range of interest for this material. In fact, Sae-Lao *et al.*³⁹ prepared

Mo/Sr multilayer coatings for the 103-154 eV region; unfortunately, multilayer reflectance significantly decreased after its exposure to air, probably due to the reactivity of Sr with oxygen and water vapour from the atmosphere.

In the calculation of k from transmittance measurements, some energy ranges for various Sr films had to be discarded. In some cases, measurements were noisy and/or the overlaps with adjacent regions were not good. But there were also cases in which one curve was not compatible with the others and hence we had to choose the ones we considered more likely to be correct. For this selection we analyzed the compatibility with the data of Henke^{31,32} and of Endriz and Spicer¹.

There was one range, 40-130 eV range, in which data of only one film (thickness of 85.0 nm) could be used, so that the slope method could not be employed. Data obtained for the other 3 films that were measured in the latter range were discarded because one of them notably deviated from calculations with Henke data and the other two data sets were erratic due to instabilities in the synchrotron facility. Where data for only one film was available we obtained initial k values through a direct calculation from transmittance measurements using Eq. (1) and neglecting reflectance ($A=0$); improved k values were calculated with the aforementioned iterative method in order to better deal with reflectance. The evaluation through sum-rules, which are presented in sub-section III-C, was also helpful in data analysis.

The above difficulties may be due mainly to the high reactivity of Sr in the residual atmosphere of the chamber even under UHV conditions.

3.2 REFRACTIVE INDEX CALCULATION THROUGH DISPERSION RELATIONS

The refractive index n of Sr was calculated using KK dispersion relations:

$$n(E) - 1 = \frac{2}{\pi} P \int_0^{\infty} \frac{E' k(E')}{E'^2 - E^2} dE' \quad (2)$$

where P stands for the Cauchy principal value. The application of Eq. (2) to calculate n requires the availability of k data over the whole spectrum, so that we extended the present data with the available data in the literature and extrapolations.

At energies smaller than the present ones, we used the data of Endriz and Spicer¹, who reported data of n and k in the 0.3-11.6 eV range. In order to get a smooth connection with Endriz's data we slightly modified our k data below 7 eV. The extrapolation to zero energy was performed by fitting a Drude model on the small energy range of Endriz's data.

At larger energies, we used Henke data from CXRO's web³⁵. At 1220 eV the connection with Henke data^{31,32} was not smooth. In order to obtain a smooth connection, we used Henke data above 1,000 eV and our data below this energy. For energies between $3 \cdot 10^4$ and $4.3 \cdot 10^5$ eV, we used the calculations of Chantler *et al.*⁴⁰. The extrapolation to infinity was performed by keeping constant the slope of the log-log plot of $k(E)$ of Chantler's data.

Fig. 5 displays k data of Sr obtained in the present research along with literature data, calculations, and extrapolations that were gathered for KK analysis. Fig. 6 displays $\delta=1-n$ calculated with Eq. (2) using the data plotted in Fig. 5; n at $N_{2,3}$, and δ at $M_{4,5}$ and $M_{2,3}$ are shown in Figs. 7 and 8, respectively. Endriz data and the semiempirical data of Henke are also displayed for comparison. There is a good qualitative agreement, although an important quantitative difference at n with respect to Endriz data, which can be due to the presence of contaminants in either set of samples and also on the different measurement techniques used: transmittance versus reflectance, the latter being more sensitive to surface roughness.

3.3 CONSISTENCY OF OPTICAL CONSTANTS

The f sum rule relates the number density of electrons to k (or to other functions); it provides a guidance to evaluate the global accuracy of k data. It is useful to define the effective number of electrons per atom $n_{eff}(E)$ contributing to k up to a given energy E ⁴¹:

$$n_{\text{eff}}(E) = \frac{4\varepsilon_0 m}{\pi N_{\text{at}} e^2 \hbar^2} \int_0^E E' k(E') dE' \quad (3)$$

where N_{at} is the atom density, e is the electron charge, ε_0 is the permittivity of vacuum, m is the electron mass, and \hbar is the reduced Planck's constant. f sum rule expresses that the high-energy limit of the effective number of electrons must reach $Z=38$, i.e., the atomic number of Sr. When the relativistic correction on scattering factors is taken into account, the high-energy limit on Eq. (3) is somewhat modified. The following modified Z was adopted here: $Z^*=37.73^{42}$. The high-energy limit that we obtained by integrating the data set plotted in Fig. 5 was 39.13, which is a 3.7% larger than the above Z^* value. The main contribution to n_{eff} was found to come from the ~ 0.7 to 10^5 eV range. Sources for the inaccuracy in Z^* may involve film thickness determination, transmittance measurement accuracy, and inconsistency in k data used in the extrapolations. The data inaccuracies mentioned in subsections 3.1 and 3.2 and the material reactivity may be other factors for this deviation.

A useful test to evaluate the accuracy of KK analysis is obtained with the inertial sum rule

$$\int_0^{\infty} [n(E) - 1] dE = 0, \quad (4)$$

which expresses that the average of the refractive index throughout the spectrum is unity. The following parameter is defined to evaluate how the integral of Eq. (4) approaches zero⁴¹:

$$\zeta = \frac{\int_0^{\infty} [n(E) - 1] dE}{\int_0^{\infty} |n(E) - 1| dE} \quad (5)$$

Shiles et al.⁴³ suggested that a good value of ζ should stand within ± 0.005 . An evaluation parameter $\zeta = 4.8 \times 10^{-4}$ was obtained here with the n data set obtained in this research. Therefore, the inertial sum rule test is well within the above top value, which along with the result for the f sum rule, suggest satisfactory consistency of n and k data.

The data are available on request at the following e-mail address: larruquert@io.cfmac.csic.es

CONCLUSIONS

The transmittance of thin films of Sr deposited by evaporation has been measured *in situ* in the 6-1220 eV photon energy range under UHV conditions. The extinction coefficient k of Sr has been calculated from transmittance measurements in the same spectral range. Sr features an absorption minimum ($k=0.029$) at ~ 18.5 eV. This relatively low absorption at this spectral range makes Sr a promising candidate for transmittance filters and reflective multilayers. A second spectral range of interest for Sr-based filters and multilayers is the low-absorption band below Sr $M_{4,5}$ edge at 132 eV. Given the high reactivity of Sr, a protective overlayer or barrier layers are expected to be required to prevent Sr from getting in contact with atmosphere or with another condensed material over the interface, respectively.

The extinction coefficient of Sr was extended both to low and to high energies from literature data and extrapolations in order to construct a self-consistent set of data. The refractive index n of Sr was obtained with KK analysis over an extended spectral range.

Current data of Sr are the first reported optical experimental data of both extinction coefficient and refractive index for condensed Sr in the whole range above 11.6 eV. The current data encompass Sr $M_{2,3}$, $M_{3,4}$, and $N_{2,3}$ edges.

The evaluation of f and inertial sum rule shows good consistency of the optical constants of Sr.

ACKNOWLEDGMENTS

We acknowledge support by the European Community - Research Infrastructure Action under the FP6 "Structuring the European Research Area" Programme (through the Integrated Infrastructure Initiative "Integrating Activity on Synchrotron and Free Electron Laser Science"). This work was also supported by the National Programme for Space Research, Subdirección General de Proyectos de

Investigación, Ministerio de Ciencia y Tecnología, project number AYA2010-22032. L. Rodríguez-de Marcos and S. García-Cortés are thankful to Consejo Superior de Investigaciones Científicas (CSIC) for funding under the Programa JAE, partially supported by the European Social Fund. M. Vidal-Dasilva acknowledges financial support from an FPI fellowship number BES-2006-14047. The technical assistance of J. M. Sánchez-Orejuela is acknowledged.

REFERENCES

- ¹ J. G. Endriz and W. E. Spicer, *Phys. Rev. B* **2**, 1466 (1970).
- ² T. Hanyu, T. Miyahara, T. Kamada, K. Asada, H. Ohkuma, H. Ishii, K. Naito, H. Kato, and S. Yamaguchi, *J. Phys. Soc. Japan* **53**, 3667 (1984).
- ³ R. Soufli, S. Bajt, and E. M. Gullikson, *Proc. SPIE* **3767**, 251 (1999).
- ⁴ M. Vidal-Dasilva, A. L. Aquila, E. M. Gullikson, F. Salmassi, and J. Larruquert, *J. Appl. Phys.* **108**, 063517 (2010).
- ⁵ Yu. Uspenski, J. Seely, N. Popov, I. Artioukov, A. Vinogradov, D. Windt, and B. Kjornrattanawanich, *Proc. SPIE* **5919**, 213 (2005).
- ⁶ B. Kjornrattanawanich, D. L. Windt, J. A. Bellotti, and J. F. Seely, *Appl. Opt.* **48**, 3084 (2009).
- ⁷ M. Fernández-Perea, J. I. Larruquert, J. A. Aznárez, J. A. Méndez, L. Poletto, D. Garoli, A. M. Malvezzi, A. Giglia, and S. Nannarone, *J. Appl. Phys.* **103**, 073501 (2008).
- ⁸ M. Fernández-Perea M. Vidal-Dasilva, , J. A. Aznárez, J. I. Larruquert, J. A. Méndez, L. Poletto, D. Garoli, A. M. Malvezzi, A. Giglia, and S. Nannarone, *J. Appl. Phys.* **103**, 113515 (2008).
- ⁹ B. Kjornrattanawanich, D. L. Windt, and J. F. Seely, *Appl. Opt.* **49**, 6006 (2010).
- ¹⁰ M. Fernández-Perea M. Vidal-Dasilva, J. A. Aznárez, J. I. Larruquert, J. A. Méndez, L. Poletto, D. Garoli, A. M. Malvezzi, A. Giglia, and S. Nannarone, *J. Appl. Phys.* **104**, 123527 (2008).

- ¹¹ M. Fernández-Perea, J. I. Larruquert, J. A. Aznárez, J. A. Méndez, L. Poletto, F. Frassetto, A. M. Malvezzi, D. Bajoni, A. Giglia, N. Mahne, and S. Nannarone, *J. Appl. Phys.* **109**, 083525 (2011).
- ¹² J. I. Larruquert, F. Frassetto, S. García-Cortés, M. Vidal-Dasilva, M. Fernández-Perea, J. A. Aznárez, J. A. Méndez, L. Poletto, A. M. Malvezzi, A. Giglia, and S. Nannarone, *Appl. Opt.* **50**, 2211 (2011).
- ¹³ M. Vidal-Dasilva, M. Fernández-Perea, J. A. Aznárez, J. I. Larruquert, J. A. Méndez, L. Poletto, A. M. Malvezzi, A. Giglia, and S. Nannarone, *J. Appl. Phys.* **105**, 103110 (2009).
- ¹⁴ J. I. Larruquert, J. A. Aznárez, J. A. Méndez, and J. Calvo-Angós, *Appl. Opt.* **42**, 4566 (2003).
- ¹⁵ M. Fernández-Perea, J. I. Larruquert, J. A. Aznárez, J. A. Méndez, L. Poletto, D. Garoli, A. M. Malvezzi, A. Giglia, and S. Nannarone, *J. Opt. Soc. Am. A* **24**, 3691 (2007).
- ¹⁶ S. García-Cortés, L. Rodríguez-de Marcos, J. I. Larruquert, J. A. Aznárez, J. A. Méndez, L. Poletto, F. Frassetto, A. M. Malvezzi, A. Giglia, N. Mahne, and S. Nannarone, *J. Appl. Phys.* **108**, 063514 (2010).
- ¹⁷ A. L. Aquila, F. Salmassi, E. M. Gullikson, F. Eriksson, and J. Birch, *Proc. SPIE* **5538**, 64 (2004).
- ¹⁸ Y. A. Uspenskii, J. F. Seely, N. L. Popov, A. V. Vinogradov, Y. P. Pershin, and V. V. Kondratenko, *J. Opt. Soc. Am. A* **21**, 298 (2004).
- ¹⁹ J. I. Larruquert, J. A. Aznárez, J. A. Méndez, A. M. Malvezzi, L. Poletto, and S. Covini, *Appl. Opt.* **43**, 3271 (2004).
- ²⁰ M. Fernández-Perea, J. I. Larruquert, J. A. Aznárez, J. A. Méndez, L. Poletto, A. M. Malvezzi, A. Giglia, and S. Nannarone, *J. Opt. Soc. Am. A* **23**, 2880 (2006).
- ²¹ B. Sae-Lao and R. Soufli, *Appl. Opt.* **41**, 7309 (2002).
- ²² M. Mansfield and J. Connerade, *Proc. R. Soc. Lond. A* **342**, 421 (1975).
- ²³ C. M. Brown, M. S. Longmire, and M. L. Ginter, *J. Opt. Soc. Am.* **73**, 985 (1983).

- ²⁴ W. R. S. Garton and K. Codling, *J. Phys. B: At. Mol. Phys.* **1**, 106 (1967).
- ²⁵ R. D. Hudson and V. L. Carter, *Phys. Rev.* **180**, 77 (1969).
- ²⁶ M. Aymar and J. M. Lecomte, *J. Phys. B* **31**, 5135 (1998).
- ²⁷ J. Langkowski, *J. Phys. D* **8**, 2058 (1975).
- ²⁸ L. Ley, N. Martensson, and J. Azoulay, *Phys. Rev. Lett.* **18**, 1516 (1980).
- ²⁹ J. Kanski and P. O. Nilsson, *Phys. Scripta* **12**, 103 (1975).
- ³⁰ W. Mende and M. Kock, *J. Phys. B* **30**, 5401 (1997).
- ³¹ B. L. Henke, P. Lee, T. J. Tanaka, R. L. Shimabukuro, and B. K. Fujikawa, *At. Data Nucl. Data Tables* **27**, 1 (1982).
- ³² B. L. Henke, E. M. Gullikson, and J. C. Davis, *Atomic Data and Nuclear Data Tables* **54**, 181 (1993).
- ³³ J. I. Larruquert, J. A. Aznárez, J. A. Méndez, A. M. Malvezzi, L. Poletto, and S. Covini, *Appl. Opt.* **43**, 3271 (2004).
- ³⁴ R. Verucchi and S. Nannarone, *Rev. Sci. Instrum.* **71**, 3444 (2000).
- ³⁵ http://www-cxro.lbl.gov/optical_constants/
- ³⁶ L. Pasquali, A. De Luisa, and S. Nannarone, *AIP Conference Proc.* **705**, 1142 (2004).
- ³⁷ S. Nannarone, F. Borgatti, A. De Luisa, B. P. Doyle, G. C. Gazzadi, A. Giglia, P. Finetti, N. Mahne, L. Pasquali, M. Pedio, G. Selvaggi, G. Naletto, M. G. Pelizzo, G. Tondello, *AIP Conference Proc.* **705**, 450 (2004).
- ³⁸ URL: <http://www.elettra.trieste.it/lightsources/elettra/elettra-beamlines/bear/research/page-7.html?showall=>
- ³⁹ B. Sae-Lao and C. Montcalm, *Opt. Lett.* **26**, 468 (2001).
- ⁴⁰ C. T. Chantler, K. Olsen, R. A. Dragoset, J. Chang, A. R. Kishore, S. A. Kotochigova, and D. S. Zucker, "X-Ray Form Factor, Attenuation and Scattering Tables" (version 2.1), (2005). [Online]

Available: <http://physics.nist.gov/ffast> [2006, May 29]. National Institute of Standards and Technology, Gaithersburg, MD. Originally published as C. T. Chantler, *J. Phys. Chem. Ref. Data* **29**, 597-1048 (2000) and C. T. Chantler, *J. Phys. Chem. Ref. Data* **24**, 71-643 (1995).

⁴¹ Altarelli and D. Y. Smith, *Phys. Rev. B* **9**, 1290 (1974).

⁴² Downloaded from the following web of Physical Reference Data, Physics Laboratory at NIST:
<http://physics.nist.gov/PhysRefData/FFast/Text/cover.html>.

⁴³ E. Shiles, T. Sasaki, M. Inokuti, and D. Y. Smith, *Phys. Rev. B* **22**, 1612 (1980).

Figure captions

Fig. 1. (color online) Log-log plot of the transmittance of Sr films with various thicknesses normalized to the transmittance of the substrate versus photon energy.

Fig. 2. (color online) Log-log plot of the extinction coefficient of Sr as a function of photon energy, along with the data of Endriz and Spicer¹, Langkowski²⁷ and Henke^{31,32}.

Fig. 3. (color online) The extinction coefficient of Sr as a function of photon energy at the small energy range, along with the data of Endriz and Spicer¹, Langkowski²⁷ and Henke^{31,32}.

Fig. 4. (color online) The extinction coefficient of Sr versus photon energy at the M_{4,5} and M_{2,3} edges, along with the data of Henke^{31,32}.

Fig. 5. (color online) Log-log plot of k data that map a wide spectral range using the current data along with the data of Endriz and Spicer¹, Henke^{31,32}, Chantler⁴⁰ and the extrapolation with a Drude model.

Fig. 6. (color online) Log-log plot of $\delta=1-n$ versus photon energy. The data of Endriz and Spicer¹, Langkowski²⁷ and Henke^{31,32} are also represented.

Fig. 7. (color online) n versus photon energy at the small energy range. The data of Endriz and Spicer¹, Langkowski²⁷ and Henke^{31,32} are also represented.

Fig. 8. (color online) $\delta=1-n$ versus photon energy at $M_{4,5}$ and $M_{2,3}$ edges. Henke data^{31,32} are also represented. There is a scale change in the abscissa axis at 150 eV.

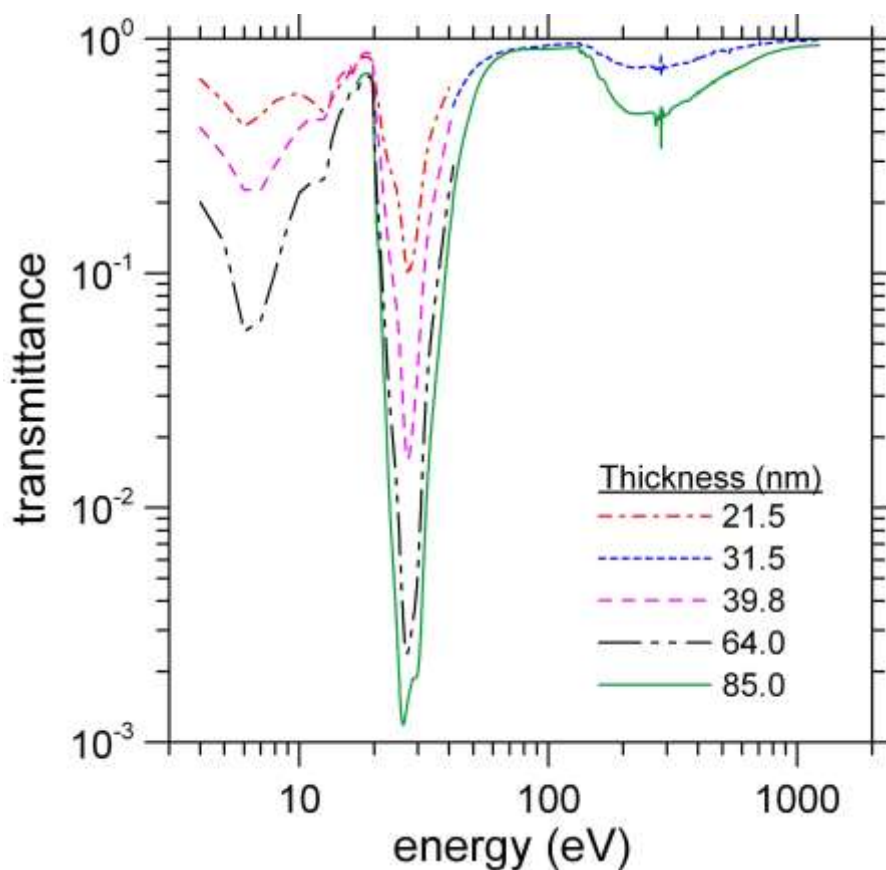


Fig. 1

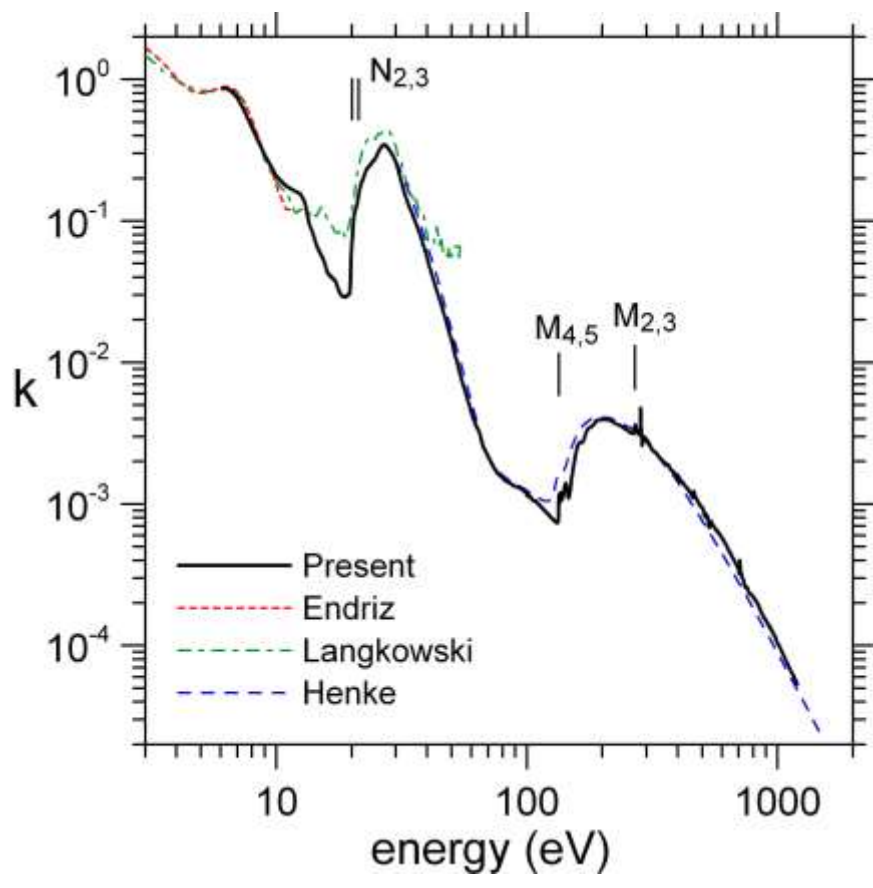


Fig. 2

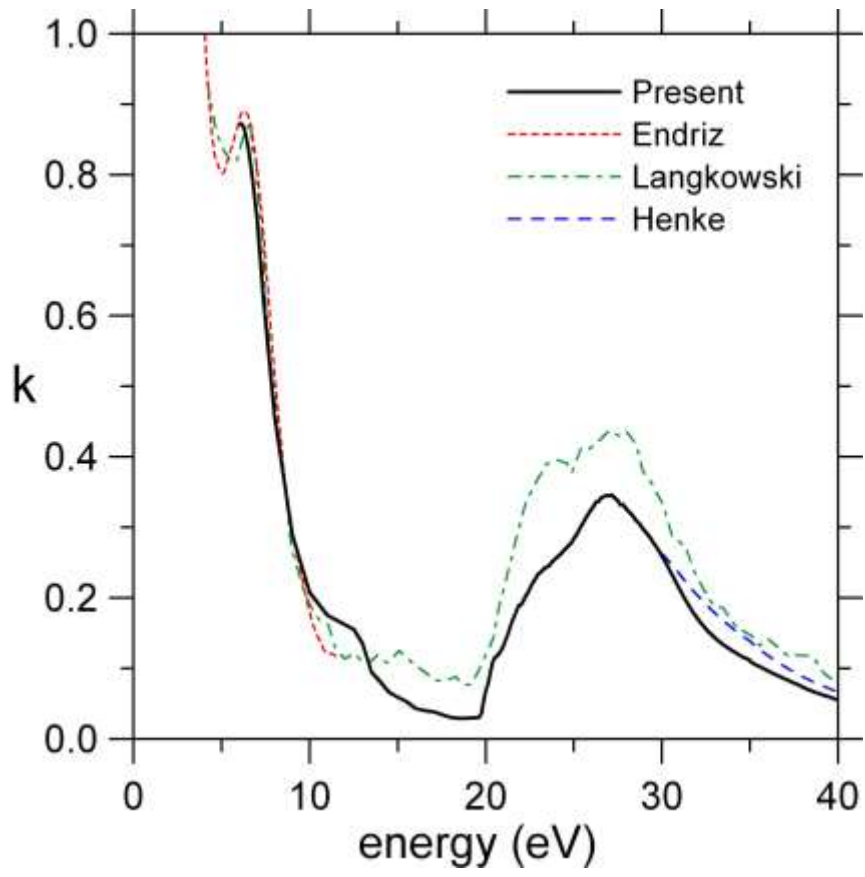


Fig. 3

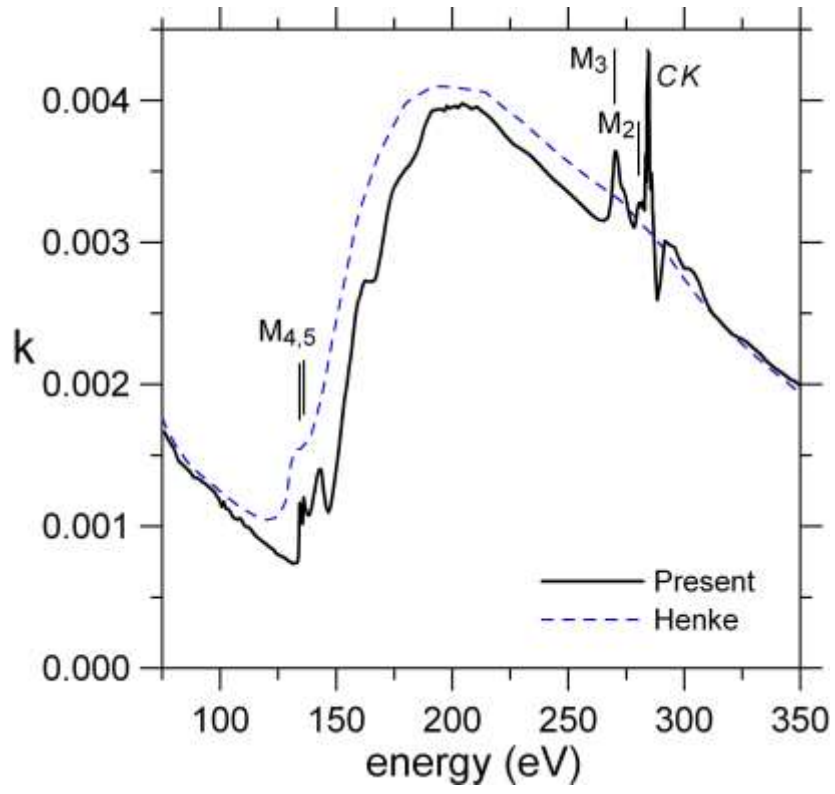


Fig. 4

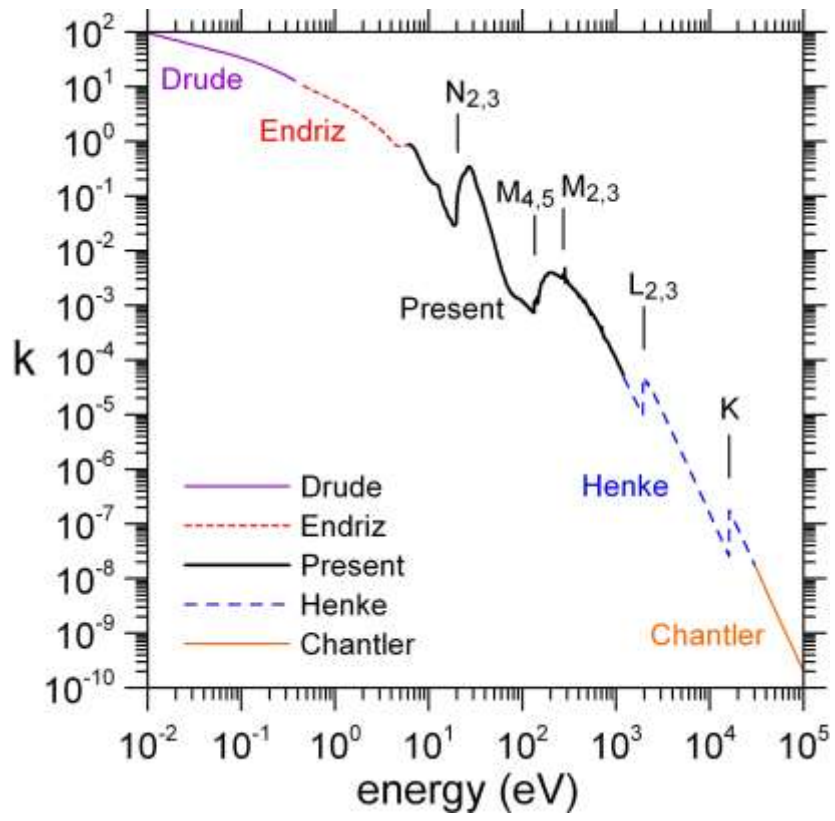


Fig. 5

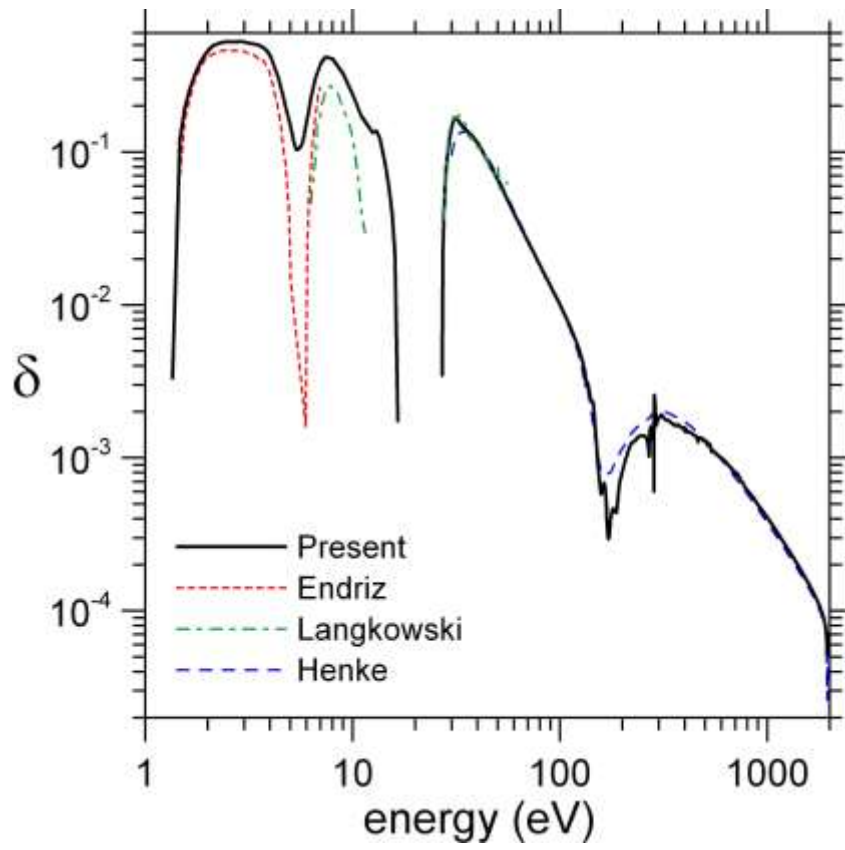


Fig. 6

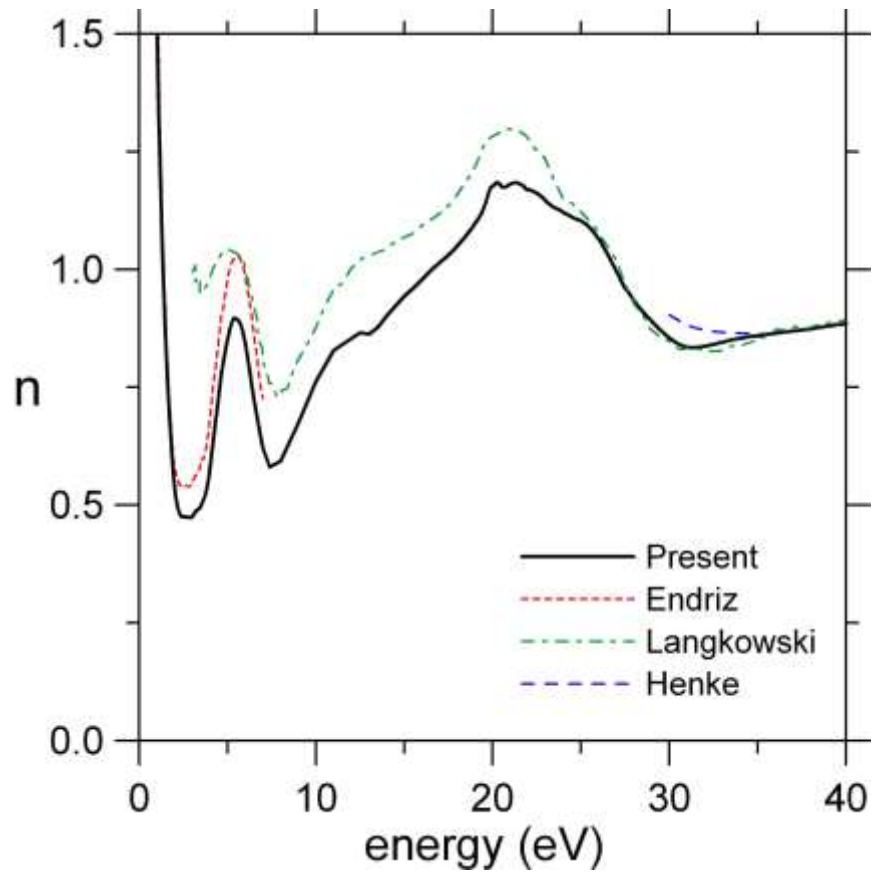


Fig. 7

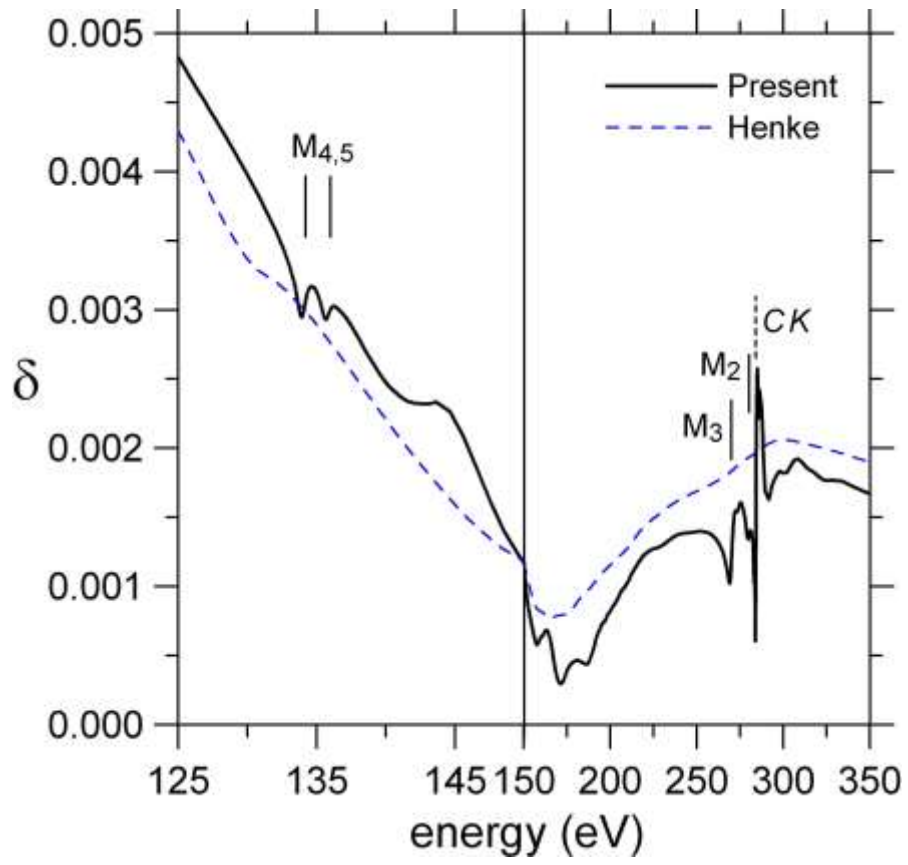


Fig. 8